

FERMI MONITORING OF RADIO-LOUD NARROW-LINE SEYFERT 1 GALAXIES

VAIDEHI S. PALIYA^{1,2}, C. S. STALIN¹, AND C. D. RAVIKUMAR²

¹Indian Institute of Astrophysics, Block II, Koramangala, Bangalore-560034, India; vaidehi@iiap.res.in

²Department of Physics, University of Calicut, Malappuram-673635, India

Received 2014 May 28; accepted 2014 October 2; published 2015 January 7

ABSTRACT

We present detailed analysis of the γ -ray flux variability and spectral properties of the five radio-loud narrow line Seyfert 1 (RL-NLSy1) galaxies, detected by the Large Area Telescope on board the *Fermi Gamma-Ray Space Telescope*, namely 1H 0323+342, SBS 0846+513, PMN J0948+0022, PKS 1502+036, and PKS 2004–447. The first three sources show significant flux variations, including the rapid variability of a few hours by 1H 0323+342. The average γ -ray spectrum of 1H 0323+342 and PMN J0948+0022 shows deviation from a simple power-law (PL) behavior, whereas the PL model gives a better fit for the other three sources. The spectra of 1H 0323+342, SBS 0846+513, and PMN J0948+0022, which are in low, flaring, and moderately active states, respectively, show significant curvature. Such curvature in the γ -ray spectrum of 1H 0323+342 and PMN J0948+0022 could be due to the emission region located inside the broad line region (BLR) where the primary mechanism of the γ -ray emission is inverse-Compton (IC) scattering of BLR photons occurring in the Klein–Nishina regime. The γ -ray emission of SBS 0846+513 is explained by IC scattering of dusty torus photons, which puts the emission region outside the BLR and thus under the Thomson regime. Therefore, the observed curvature of SBS 0846+513 could be intrinsic to the particle energy distribution. The presence of curvature in the γ -ray spectrum and flux variability amplitudes of some of the RL-NLSy1 galaxies suggests that these sources could be akin to low/moderate jet power flat spectrum radio quasars.

Key words: galaxies: active – galaxies: jets – galaxies: peculiar – galaxies: Seyfert – gamma rays: galaxies – quasars: individual (1H 0323+342, SBS 0846+513, PMN J0948+0022, PKS 1502+036, PkS 2004-447)

Supporting material: data behind figure

1. INTRODUCTION

The launch of the *Fermi Gamma-Ray Space Telescope* (*Fermi*) in 2008 has led to the discovery of γ -ray emission in a large number of blazars—comparable to that found by the *Energetic Gamma-Ray Experiment Telescope* (*EGRET*; Thompson et al. 1993)—owing to its large sensitivity and wide energy coverage. This has clearly demonstrated that blazars dominate the population of γ -ray emitters for which classification is known (Nolan et al. 2012). Interestingly, *Fermi* has also observed variable γ -ray emission from some radio-loud narrow line Seyfert 1 (RL-NLSy1) galaxies (Abdo et al. 2009c, 2009d; Calderone et al. 2011; D’Ammando et al. 2012). First identified as a new class of active galactic nuclei (AGNs) by Osterbrock & Pogge (1985), NLSy1 galaxies have narrow Balmer lines (FWHM (H_β) $< 2000 \text{ km s}^{-1}$), weak [O III] ($[\text{O III}]/H_\beta < 3$) and strong optical Fe II lines (Osterbrock & Pogge 1985; Goodrich 1989). They also possess soft X-ray excess (Boller et al. 1996; Wang et al. 1996; Leighly 1999a), relatively low black hole (BH) mass ($\sim 10^6 - 10^8 M_\odot$), high accretion rate (Peterson et al. 2000; Hayashida 2000; Grupe & Mathur 2004; Zhou et al. 2006; Xu et al. 2012), and rapid X-ray flux variations (Pounds et al. 1995; Leighly 1999b). They also exhibit the radio-quiet/radio-loud dichotomy (Laor 2000), and $\sim 7\%$ NLSy1 galaxies are found to be radio-loud (Komossa et al. 2006), which is a lesser fraction when compared to the $\sim 15\%$ found in a quasar population (Urry & Padovani 1995). Some of these RL-NLSy1 galaxies show a compact core-jet structure, high brightness temperature, and superluminal behavior (Komossa et al. 2006; Doi et al. 2006). Kiloparsec scale radio structures are also reported in some RL-NLSy1

galaxies (Antón et al. 2008; Doi et al. 2012). These characteristics indicate the presence of aligned relativistic jets in RL-NLSy1 galaxies, and this was confirmed via the detection of γ -ray emission from five RL-NLSy1 galaxies by the Large Area Telescope (LAT) on board *Fermi* (Abdo et al. 2009c, 2009d; D’Ammando et al. 2012). Recently, high and variable optical polarization and rapid optical/infrared flux variations were observed in some of these γ -ray emitting NLSy1 (γ -NLSy1) galaxies (Liu et al. 2010; Ikejiri et al. 2011; Jiang et al. 2012; Itoh et al. 2013; Paliya et al. 2013a). Modeling the spectral energy distribution (SED) of γ -NLSy1 galaxies led to the conclusion that they possess a characteristic double hump SED similar to blazars, and the physical properties of these sources are intermediate to the other two members of the blazar family, namely BL Lac objects and flat spectrum radio quasars (FSRQs; Abdo et al. 2009d; Foschini et al. 2011b; D’Ammando et al. 2012; Paliya et al. 2013b). In addition, Foschini et al. (2010) showed that one of these γ -NLSy1 galaxies, PMN J0948+0022, occupies an intermediate position in the well-known blazar sequence (Fossati et al. 1998). Although many properties of γ -NLSy1 galaxies are similar to those of blazars, there also exist characteristic differences. For example, blazars are known to be hosted by massive elliptical galaxies (Marscher 2009) whereas the γ -NLSy1 galaxies, which are similar to other NLSy1 galaxies, are likely to be hosted by spiral galaxies with relatively low-mass BHs at their centers (León Tavares et al. 2014). Therefore, detailed studies of these γ -NLSy1 galaxies will enable us understand the physical properties of relativistic jets at different mass and accretion rate scales. Also, a clear understanding of the shape of the observed γ -ray spectrum can help us place constraints on the various models proposed to

Table 1
Basic Information of the γ -NLSy1 Galaxies Studied in This Work

Name	R.A. (2000) (h m s)	Decl. (2000) (d m s)	z	V (mag)	α_R	R	$\text{Log } M_{\text{BH}}$ (M_{\odot})	References for M_{BH}
1H 0323+342	03:24:41.2	+34:10:45	0.063	15.72	-0.35	318	7.0	Zhou et al. (2006)
SBS 0846+513	08:49:58.0	+51:08:28	0.584	18.78	-0.26	4496	7.4	Yuan et al. (2008)
PMN J0948+0022	09:48:57.3	+00:22:24	0.584	18.64	0.81	846	7.5	Yuan et al. (2008)
PKS 1502+036	15:05:06.5	+03:26:31	0.409	18.64	0.41	3364	6.6	Yuan et al. (2008)
PKS 2004-447	20:07:55.1	-44:34:43	0.240	19.30	0.38	6358	6.7	Oshlack et al. (2001)

explain the high-energy component present in broadband SED of these sources.

In this work we present γ -ray flux variability properties and γ -ray spectral properties of five γ -NLSy1 galaxies using \sim five years of *Fermi*-LAT data. Wherever possible, we also study their γ -ray spectral behavior in different activity states. The motivation here is to see the similarities and/or differences in the γ -ray spectra and the γ -ray flux variability of these sources with respect to the blazar class of AGN, which emits copiously in the γ -ray band.

The paper has been organized as follows. Sample selection is discussed in Section 2. Section 3 is devoted to data reduction and analysis procedures. We discuss the results in Section 4, followed by our conclusions in Section 5. Throughout the work, we adopt $\Omega_m = 0.27$, $\Omega_{\Lambda} = 0.73$ and $H_0 = 71 \text{ km s}^{-1} \text{ Mpc}^{-1}$.

2. SAMPLE

As of now (2014 September 1), five RL-NLSy1 galaxies are found to be emitting in the γ -ray band by *Fermi*-LAT with high significance, having test statistic (TS) > 25 ($\sim 5\sigma$; Mattox et al. 1996). General information about these five γ -NLSy1 galaxies is given in Table 1. In Table 1, the values of right ascension, declination, redshift, and the apparent V -band magnitude are taken from Véron-Cetty & Véron (2010). The given radio spectral indices are calculated using the 6 cm and 20 cm flux densities found in Véron-Cetty & Véron (2010; $S_{\nu} \propto \nu^{\alpha}$), and the values of the radio loudness parameter R^3 are taken from Foschini (2011).

3. DATA REDUCTION AND ANALYSIS

The observational data used in this work were collected by *Fermi*-LAT (Atwood et al. 2009) over the first five years of its operation, from 2008 August 5 (MJD 54,683) to 2013 November 1 (MJD 56,597). Standard procedures described in the *Fermi*-LAT documentation are used to analyze the data. We use *ScienceTools* v9r32p5 along with the post-launch instrument response functions (IRFs) P7REP_SOURCE_V15. In the energy range of 0.1–300 GeV, only the events belonging to the SOURCE class are selected. To avoid contamination from Earth limb γ -rays, source events coming from zenith angle $< 100^\circ$ are extracted. The filters DATA_QUAL==1, LAT_CONFIG==1, and ABS(ROCK_ANGLE)<52 are used to select the good time intervals. To model the background, a galactic diffuse emission component (gll_iem_v05.fits) and an isotropic component iso_source_v05.txt⁴ are considered. While fitting the five-year average spectrum, the normalization of components in the background model and the photon index of the galactic diffusion

model are allowed to vary freely. We fix these parameters to the values obtained from the fitting during the subsequent time series analysis.

To evaluate the significance of the γ -ray signal, we use the maximum-likelihood (ML) $\text{TS} = 2\Delta \log(\text{likelihood})$ between models with and without a point source at the position of the source of interest. We use the binned likelihood method to generate the average γ -ray spectrum, as well as the spectra over different time periods. The source model includes all point sources from the second *Fermi*-LAT catalog (2FGL; Nolan et al. 2012) that lie within the 15° region of interest (ROI) of every source. Many sources are detected by *Fermi*-LAT after the release of the 2FGL catalog (see, e.g., Gasparrini & Cutini 2011) and thus are not included. However, if these newly detected sources lie in the vicinity of a source of interest, they could have an effect on the results of the analysis. Thus we search for possible new sources within the ROI of the five γ -NLSy1 galaxies studied here by generating their residual TS map using the tool *gttsmap*. These residual TS maps are shown in Figure 1. Using the criterion $\text{TS} > 25$, we find two un-modeled sources associated with each of the residual TS maps of 1H 0323+342 (R.A., decl. = 48:236, 36:260 and 56:092, 32:804; J2000) and PKS 2004-447 (R.A., decl. = 307:257, -42:592 and 307:505, -41:542; J2000), and one source each in the residual TS maps of SBS 0846+513 (R.A., decl. = 133:112, 55:497; J2000) and PMN J0948+0022 (R.A., decl. = 142:854, 0:497; J2000). No new source with $\text{TS} > 25$ is seen in the residual TS map of PKS 1502+036. These new sources are then modeled by a power law (PL) and are included in our analysis. However, we note that because they are faint, the inclusion of these new sources has a negligible effect on the results that were obtained without them. Further, both PL and log parabola (LP) models are used to parameterize the γ -ray spectra of the sources. For objects that fall within 7° of each of the target sources studied here, all parameters except the scaling factor are allowed to vary for the sources that lie between 7° – 14° and only the normalization factor is allowed to vary freely. For the remaining sources that lie outside 14° , all parameters are fixed to the values given in the 2FGL catalog. We perform a first run of the ML analysis and then remove all sources from the model with $\text{TS} < 25$. This updated model is then used to carry out a second ML analysis. If the likelihood fitting shows non-convergence, all parameters of the sources lying outside 7° from the center of the ROI are fixed to the values obtained from the average likelihood fitting, and the fitting is repeated. In cases where we find that the fitting shows non-convergence, we repeat it by fixing the photon indices of the sources further 1° inside the edge of the ROI. This process is carried out iteratively until the analysis converges. To

³ Defined as the ratio of flux density in 5 GHz to that in the optical B band.

⁴ <http://fermi.gsfc.nasa.gov/ssc/data/access/lat/BackgroundModels.html>

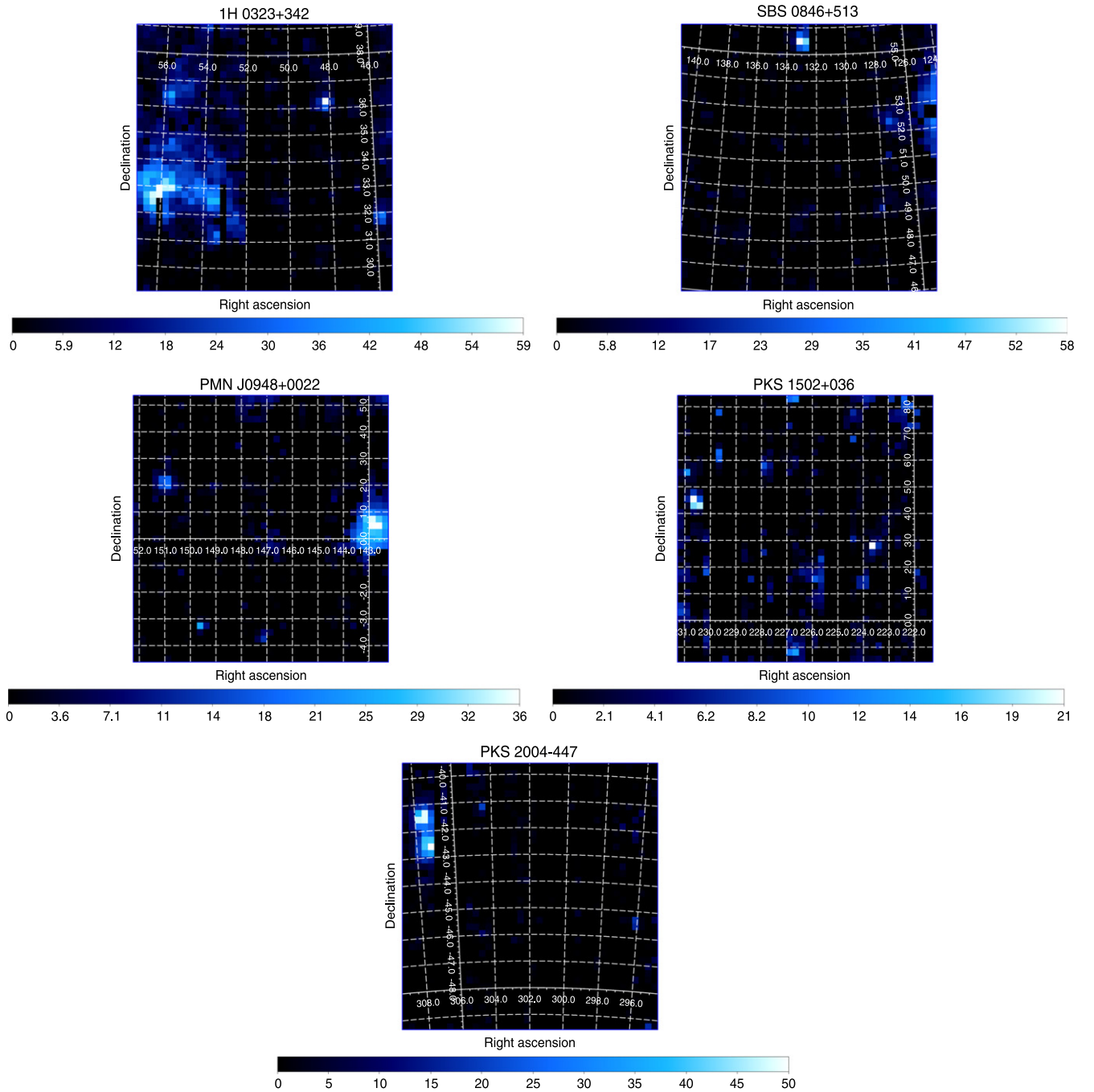


Figure 1. Residual TS maps of the 0.1–300 GeV events during the time period covered in this work, centered on the coordinates of the γ -NLSy1 galaxies. There are two new sources each in the TS maps of 1H 0323+342 and PKS 2004–447, and one new source each in the TS maps of SBS 0846+513 and PMN J0948+0022. We do not find any new sources in the TS map of PKS 1502+036.

generate weekly binned light curves, we use a PL model for all γ -NLSy1 galaxies, because the PL indices obtained from this model show smaller statistical uncertainties when compared to those obtained from fits using more complex models. To generate daily averaged and six-hour binned light curves, only the normalization parameter of the source of interest is kept free and the rest of the parameters are fixed to the values obtained from the five-year averaged fitting. In all the cases (i.e., for the light curve as well as spectrum generation), we consider the source to be detected at the $\sim 3\sigma$ level (e.g., Kraft et al. 1991) if the condition $TS > 9$ is satisfied in the respective time or energy bin. We calculate 2σ upper limits whenever $\Delta F_\gamma/F_\gamma > 0.5$ and/or $1 < TS < 9$,

where ΔF_γ is the 1σ error estimate in the γ -ray flux F_γ . This is found by varying the flux of the source given by `gtlike`, until the TS reaches a value of four (e.g., Abdo et al. 2010b). The upper limits are not calculated for $TS < 1$. Primarily governed by the uncertainty in the effective area, the measured fluxes have energy dependent systematic uncertainties of around 10% below 100 MeV, 5% between 316 MeV and 10 GeV, and 10% above 10 GeV.⁵ Unless otherwise specified, all the errors quoted in this paper are 1σ statistical uncertainties.

⁵ http://fermi.gsfc.nasa.gov/ssc/data/analysis/LAT_caveats.html

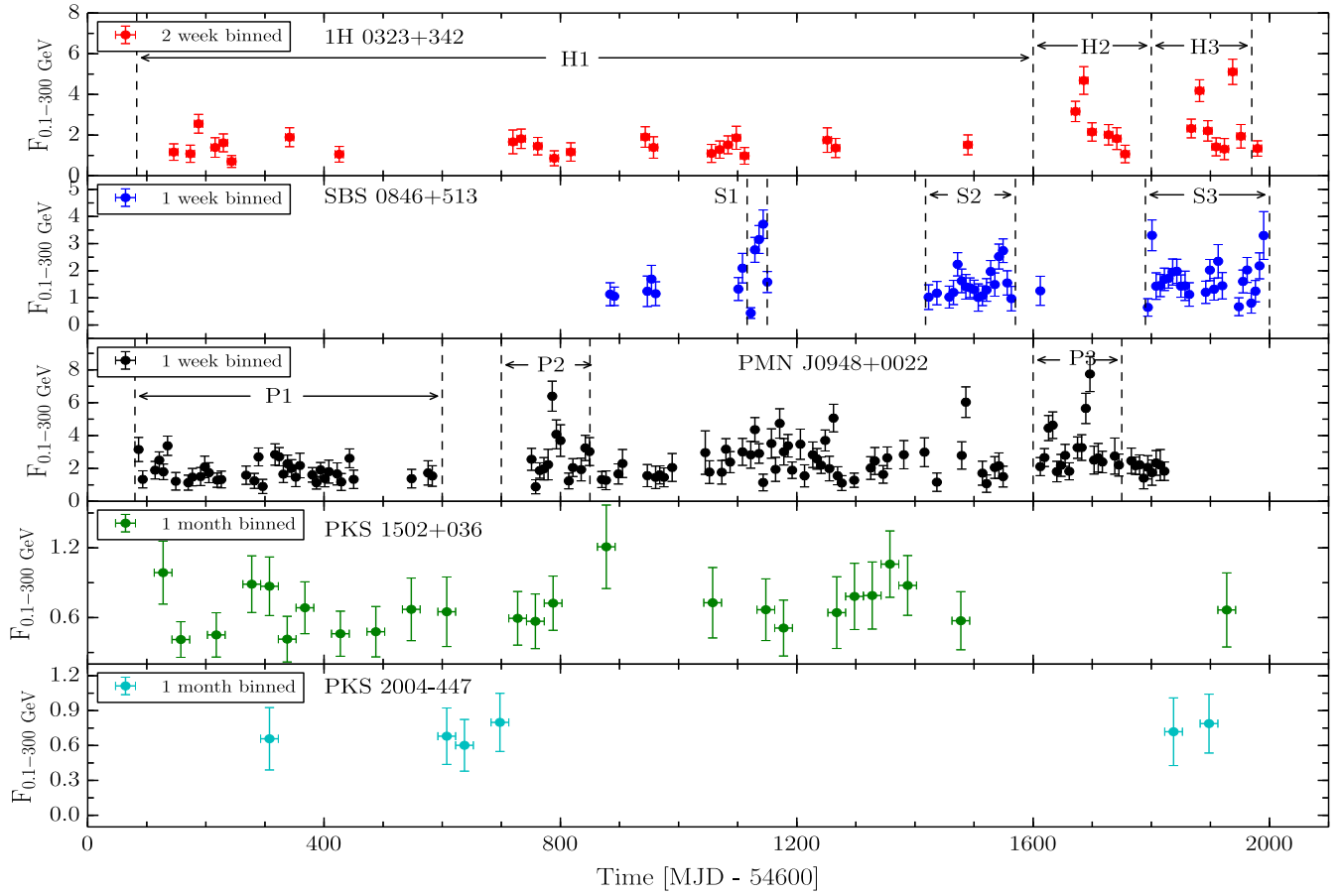


Figure 2. Long-term γ -ray light curves of the γ -NLSy1 galaxies. Flux values are in units of 10^{-7} ph cm^{-2} s^{-1} . MJD 54,600 corresponds to 2008 May 14. Different activity periods are marked with the appropriate notations. See text for details. The data used to create this figure are available.

Table 2

Fractional rms Variability and Variability Probability of the γ -NLSy1 Galaxies

Name	Binning (days)	F_{var}	Probability (%)
1H 0323+342	14	0.498 ± 0.046	>99.0
SBS 0846+513	7	0.467 ± 0.042	>99.0
PMN J0948+0022	7	0.443 ± 0.029	>99.0
PKS 1502+036	30	...	34.5
PKS 2004-447	30

4. RESULTS AND DISCUSSION

4.1. Long-term Flux Variability

The γ -ray light curves of the five γ -NLSy1 galaxies obtained using the procedures outlined in Section 3 are shown in Figure 2. Depending on the γ -ray brightness, different time bins are used for different objects. For clarity, we have not shown upper limits. Variability in the light curve is tested by calculating fractional rms variability (F_{var}) and variability probability by means of a simple χ^2 test, using the recipes of Vaughan et al. (2003) and Abdo et al. (2010c), respectively. The results are shown in Table 2.

The bi-weekly binned light curve of 1H 0323+342 shows that it is nearly steady in γ -rays during the initial four years of the LAT observations, however, it displays flaring behavior at two epochs in 2013—one around MJD 56,300 and the other around MJD 56,500. These are marked as H2 and H3 in Figure 2. The F_{var} for this source is 0.498 ± 0.046 , which is on

the higher side of that obtained for FSRQs ($\sim 0.24 \pm 0.01$) by Abdo et al. (2010c), thus indicating substantial flux variations. The probability that the source has shown variation is >99% (see Table 2). The average γ -ray flux during most of its quiescence is $\sim 8 \times 10^{-8}$ ph cm^{-2} s^{-1} . A maximum γ -ray flux of $(5.11 \pm 0.62) \times 10^{-7}$ ph cm^{-2} s^{-1} is observed in the bin centered at MJD 56,537 when a GeV flare was detected by *Fermi*-LAT (Carpenter & Ojha 2013; Paliya et al. 2014). The five-year averaged TS value of this source is ~ 723 , which corresponds to $\sim 27\sigma$ detection.

SBS 0846+513 was in quiescence during the first two years of *Fermi* operation and thus was not included in the 2FGL catalog. This source was discovered in the γ -ray band only when *Fermi*-LAT detected a flare in 2011 (Foschini 2011). After that, many flaring activities have been observed from this source and they are shown by S1, S2, and S3 in Figure 2. A flux of $\sim 4 \times 10^{-8}$ ph cm^{-2} s^{-1} and TS ~ 1700 is obtained from the average analysis. The probability that this source is variable is >99% and shows a value of 0.467 ± 0.042 to the F_{var} .

PMN J0948+0022 is the first RL-NLSy1 galaxy detected in the γ -ray band by *Fermi*-LAT. An average analysis of \sim five years of the LAT data gives the γ -ray flux and TS of $\sim 1.3 \times 10^{-7}$ ph cm^{-2} s^{-1} and ~ 3300 , respectively. From its weekly binned light curve, the peak flux value of $(7.74 \pm 1.07) \times 10^{-7}$ ph cm^{-2} s^{-1} is observed during a recent GeV flare (D’Ammando & Orienti 2013). The ratio of the maximum to minimum flux is ~ 17 , which is significantly higher than that noticed by Foschini et al. (2012). The primary reason for this

difference is the time ranges covered by the analyses. The peak flux is observed in the bin centered at MJD 56,297, which is not covered by Foschini et al. (2012). Few significant flaring activities are observed and we consider two of them for further analysis. These flaring periods are noted as P2 and P3 in Figure 2. We find a value of F_{var} for 0.443 ± 0.029 , which clearly hints at the existence of substantial flux variability in this source.

PKS 1502+036 has been detected by *Fermi*-LAT most of the time, however, it is at a low flux level of $\sim 4.5 \times 10^{-8}$ ph cm $^{-2}$ s $^{-1}$, as can be seen in the monthly binned light curve in Figure 2. The five-year average analysis gives a TS value of ~ 435 , which corresponds to $\sim 20\sigma$ detection. When comparing the results obtained here with that of D’Ammando et al. (2013b), the average flux and photon index values are found to be quite similar, despite the fact that we have included one more year of the LAT data than they did. The similarity seen in both analyses can be justified by the fact that PKS 1502+036 is hardly detected by *Fermi*-LAT in the period MJD 56,235–56,597 (see the third panel from top in Figure 2), which they do not cover. The χ^2 analysis classifies the source to be a non-variable.

PKS 2004–447 has the lowest values for the γ -ray flux ($1.42 \pm 0.24 \times 10^{-8}$ ph cm $^{-2}$ s $^{-1}$) and the TS (106) among γ -NLSy1 galaxies, and was detected by *Fermi*-LAT only on a few occasions. Hence no definite conclusion can be drawn about its flux variability behavior owing to the low photon statistics because we could not get a significant value for the F_{var} .

4.2. Short-term Flux Variability and Jet Energetics

Blazars are known to vary on sub-hour timescales (e.g., Foschini et al. 2011a; Saito et al. 2013) and this could constrain the size and location of the γ -ray emitting region (see e.g., Tavecchio et al. 2010; Brown 2013). We therefore search for the presence of flux variability over short timescales (of the order of hours) in the light curves of the γ -NLSy1 galaxies. From the long-term light curves of 1H 0323+342, SBS 0846+513, and PMN J0948+0022, we identify the epochs of high activity (shown in Figure 2) and generate one day and six hour binned light curves. We then scan the data to calculate the shortest flux doubling/halving timescale using the following equation:

$$F(t) = F(t_0) \cdot 2^{(t-t_0)/\tau},$$

where $F(t)$ and $F(t_0)$ are the fluxes at time t and t_0 , respectively, and τ is the characteristic doubling/halving timescale. We also set the condition that the difference in flux at the epochs t and t_0 is at least significant at the 3σ level (Foschini et al. 2011a).

The recent GeV flare detected from 1H 0323+342 (Carpenter & Ojha 2013) had a daily γ -ray flux as high as $(1.75 \pm 0.33) \times 10^{-6}$ ph cm $^{-2}$ s $^{-1}$, which is ~ 23 times larger than the five-year average flux. The photon statistics during this epoch (2013 August 28–2013 September 1) are good enough to generate a six-hour binned light curve (see Figure 3). In contrast to the earlier observations where γ -ray variability of the γ -NLSy1 galaxies were characterized over longer timescales (≥ 1 day; e.g., Calderone et al. 2011; Foschini et al. 2012), this epoch of high activity provides evidence of extremely fast variability observed from a γ -NLSy1 galaxy. A flux-doubling time as small as 3.09 ± 0.85 hours (assuming an exponential rise of the flare) is the fastest

γ -ray variability ever observed from this class of AGN. In the time bin when the highest flux is measured, the TS value is 136 associated with a registered count of 34. The flux doubling time obtained here is significantly different from the value of 3.3 ± 2.5 days reported by Calderone et al. (2011) using an e-folding timescale. The primary reason for this contrast is the fact that 1H 0323+342 was in quiescence for most of the first four years of *Fermi* operation and could not produce enough photon statistics to study short timescale variability. These findings are similar to what was recently reported by Paliya et al. (2014). The highest flux in the six-hour binned light curve is measured as $(7.80 \pm 1.43) \times 10^{-6}$ ph cm $^{-2}$ s $^{-1}$, which corresponds to an isotropic γ -ray luminosity of 2.82×10^{46} erg s $^{-1}$, which is ~ 100 times higher than the five-year average value. The total power radiated in the γ -ray band (Sikora et al. 1997), thus, would be $L_{\gamma,\text{em}} \simeq L_{\gamma,\text{iso}}/2\Gamma^2 \simeq 2.20 \times 10^{44}$ erg s $^{-1}$ (assuming a bulk Lorentz factor $\Gamma = 8$; Paliya et al. 2014), which is approximately 16% of the Eddington luminosity considering a BH mass of $10^7 M_{\odot}$ (Zhou et al. 2006).

Detection of a large flare in 2011 June led to the discovery of SBS 0846+513 in the γ -ray band. During this period of high activity we find a maximum daily averaged flux of $(8.20 \pm 0.08) \times 10^{-7}$ ph cm $^{-2}$ s $^{-1}$, which is almost 20 times higher than the five-year average flux. When the data are further re-binned using six-hour bins, we notice a high γ -ray flux of $(9.37 \pm 1.74) \times 10^{-7}$ ph cm $^{-2}$ s $^{-1}$. The apparent isotropic γ -ray luminosity is found to be $\sim 1.44 \times 10^{48}$ erg s $^{-1}$. Blazars, in general, and FSRQs in particular, are known to be emitters of such high power in the γ -ray band. If a bulk Lorentz factor of 15 (D’Ammando et al. 2012) is assumed, we estimate that the total radiated power in γ -rays would be $L_{\gamma,\text{em}} \simeq 3.21 \times 10^{45}$ erg s $^{-1}$, which is about 93% of the Eddington luminosity assuming a BH mass of $10^{7.4} M_{\odot}$ (Yuan et al. 2008), a value generally found for powerful FSRQs (e.g., Nemmen et al. 2012). We find many instances during this flaring period when the apparent isotropic γ -ray luminosity exceeds 10^{48} erg s $^{-1}$ (e.g., MJD 55,742 and 55,745). During the GeV flare in 2011 June, we find the shortest flux-halving timescale of $\sim 25.6 \pm 11.0$ hours.

PMN J0948+0022 is the most γ -ray luminous NLSy1 galaxy ever detected by *Fermi*-LAT. During its recent GeV flare (D’Ammando & Orienti 2013) we observe a maximum one-day average flux of $(1.76 \pm 0.32) \times 10^{-6}$ ph cm $^{-2}$ s $^{-1}$ on MJD 56,293, which is about 14 times the five-year average value and the highest daily binned flux observed from the source in our analysis. The highest one-day binned flux is similar to that noted by Foschini et al. (2012). On further dividing this active period into six-hour bins, we find a maximum flux value of $(2.40 \pm 0.83) \times 10^{-6}$ ph cm $^{-2}$ s $^{-1}$. This corresponds to an isotropic γ -ray luminosity of 1.87×10^{48} erg s $^{-1}$, which is ~ 20 times its five-year average value. The total radiated power in the γ -ray band is $L_{\gamma,\text{em}} \simeq 4.16 \times 10^{45}$ erg s $^{-1}$ (assuming a bulk Lorentz factor of $\Gamma = 15$). If its BH mass is assumed to be $10^{7.5} M_{\odot}$ (Yuan et al. 2008), then we find that the radiated γ -ray power is $\sim 95\%$ of the Eddington luminosity. The shortest timescale of variability observed from this source is found to be 74.7 ± 27.6 hours, which is comparable to that reported by Foschini et al. (2012) and Calderone et al. (2011).

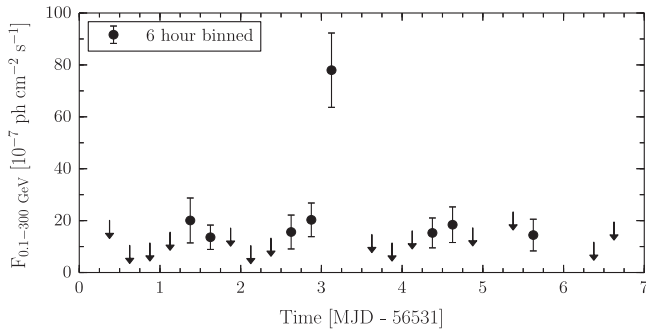


Figure 3. Six-hour binned γ -ray light curve of 1H 0323+342 covering the period of the GeV outburst. Upper limits at the 2σ level are shown by downward arrows.

4.3. Gamma-ray Spectrum

The analysis of the γ -ray spectral shape is done using two spectral models: PL ($dN/dE \propto E^{-\Gamma_\gamma}$), where Γ_γ is the photon index, and LP ($dN/dE \propto (E/E_o)^{-\alpha-\beta \log(E/E_o)}$), where E_o is the reference energy that is fixed at 300 MeV, α is the photon index at E_o , and β is the curvature index that defines the curvature around the peak. The low-photon statistics of all the sources precludes us to analyze the γ -ray spectral shape using more complex models, such as broken power law (BPL) or PL with exponential cut-off. The spectral analysis is performed using a binned ML estimator `gtlike` following the prescription given in Section 3. We use a likelihood ratio test (Mattox et al. 1996) to check the PL model (null hypothesis) against the LP model (alternative hypothesis). Following Nolan et al. (2012), TS of the curvature $TS_{\text{curve}} = 2(\log L_{\text{LP}} - \log L_{\text{PL}})$ is also calculated. The presence of a significant curvature is tested by setting the condition $TS_{\text{curve}} > 16$.

4.3.1. Average Spectral Analysis

The results of the average spectral analysis of the five γ -NLSy1 galaxies using five years of *Fermi*-LAT data are tabulated in Table 3. Two sources, 1H 0323+342 and PMN J0948+0022, are found to have a significant curvature in their γ -ray spectrum. The value of TS_{curve} reported in Table 3 shows that the LP model describes their spectrum better than the PL model. A TS_{curve} value of ~ 15 for SBS 0846+513 indicates a possible curvature in its γ -ray spectrum. For the remaining two sources no significant curvature is noticed. This may be due to low photon statistics. However, in the future when more γ -ray data is accumulated, it is likely that they will also show a significant deviation from the PL model. To show the departure from a PL behavior, and for better visualization of the spectral shape, we perform a binned likelihood analysis on appropriately chosen energy bins covering 0.1–300 GeV and generate the SED. The results are shown in Figure 4. Since there is no signal beyond 30 GeV, the γ -ray spectra are only shown up to 30 GeV. In this figure, the solid red line represents the PL model, and the LP model is plotted by a green dashed line. From the residual plot (lower panel) of the PL model fits to the sources, it is evident that the spectrum of 1H 0323+342 and PMN J0948+0022 clearly deviate from the PL behavior, confirming the TS_{curve} test. In addition, hints of curvature can be seen in the residual plot of SBS 0846+513. PMN J0948+0022 has the most prominent curvature in its γ -ray spectrum ($\sim 8\sigma$), whereas a $\sim 4\sigma$ significant curvature is noticed in the

spectrum of 1H 0323+342. Further, the curvature index β for PKS 2004–447 is found to be high and does not appear to be realistic because no significant curvature is found in the γ -ray spectrum of this source. Thus, the unusual β value may be indicating the poor photon statistics associated with the observation and hence seems unreliable.

4.3.2. Spectral Analysis of Low and High Activities

Of the five γ -NLSy1 galaxies in our sample, three sources—1H 0323+342, SBS 0846+513, and PMN J0948+0022—are relatively bright and have shown GeV flaring activities (e.g., Donato 2010; Donato & Perkins 2011; Carpenter & Ojha 2013), thus enabling us to probe their spectral behavior at different activity states. From the light curves, we identify periods when the sources are found to be in relatively low and high states. These periods are marked in Figure 2. A high activity state refers to the period of detection of high flux by the LAT, as already reported in the literature. A low activity state is selected to be the time period when the source is in a relatively fainter state. We note that the low activity states may not represent the actual quiescence of the sources. The idea here is to compare the spectral shapes at different activity periods, so selecting true quiescence would not serve the purpose due to poor photon statistics. Many GeV flares from PMN J0948+0022 have been reported (Donato 2010; D’Ammando & Cipriani 2011; D’Ammando & Orienti 2013) and we select the two brightest (P2 and P3) for further analysis. The time duration along with the results of the likelihood analysis are presented in Table 4. For better visualization, we also show the spectra of the sources along with their best-fit model in Figures 5 and 6. A statistically significant ($\sim 4\sigma$) curvature is noticed in the low activity state γ -ray spectrum of 1H 0323+342. Interestingly, no curvature is found in the high-activity states of this source. A substantial curvature ($\sim 5\sigma$) is noticed in the first flaring state (S1) of SBS 0846+513, which is similar to that reported by D’Ammando et al. (2012). No curvature is found in the other flaring state of this source (period S2; MJD 56,018–56,170), whereas for the same period D’Ammando et al. (2013a) detected curvature. A curvature is also noticed in the low activity state (P1) of PMN J0948+0022, but not during the GeV outbursts. This behavior is in contrast to that observed in bright blazars 3C 454.3 and PKS 1510–089, where a significant curvature is detected in their γ -ray spectra during the outbursts (Abdo et al. 2010a, 2011).

4.3.3. Spectral Evolution

We now investigate the changes in the spectra in relation to the brightness of the γ -NLSy1 galaxies. Instead of attempting to provide the best description of a spectrum, we intend to search for possible trends. Hence, we evaluate the PL spectral indices during the time bins used for the light curves shown in Figure 2. The spectral index can be considered to be a representative of the mean slope.

The photon index of 1H 0323+342 is found to be harder in the high-activity states. For example, in the bin centered at MJD 56,285 (peak flux in the interval H2 in Figure 2), the photon index value of 2.51 ± 0.12 is significantly harder than the value of 2.78 ± 0.05 found for the five-year average. A hard photon index value of 2.49 ± 0.11 is also found during the 2013 August GeV outburst. Similar behavior is also seen in SBS 0846+513. During its first GeV outburst, which led to the

Table 3
Details of the PL and LP Model Fits to the Five-year Average γ -ray Data of the γ -NLSy1 Galaxies

Name	PL				LP					
	Γ_γ	$F_{0.1-300 \text{ GeV}}^a$	TS	$\text{Log } L_{\text{PL}}^b$	α	β	$F_{0.1-300 \text{ GeV}}^a$	TS	$\text{Log } L_{\text{LP}}^b$	TS_{curve}
1H 0323+342	2.78 ± 0.05	7.54 ± 0.39	732.3	44.4	2.66 ± 0.06	0.19 ± 0.05	6.98 ± 0.40	738.3	44.3	17.36
SBS 0846+513	2.26 ± 0.03	4.35 ± 0.22	1666.9	46.7	2.04 ± 0.07	0.09 ± 0.03	3.73 ± 0.27	1660.4	46.7	15.03
PMN J0948+0022	2.62 ± 0.02	13.03 ± 0.36	3299.8	47.0	2.35 ± 0.04	0.20 ± 0.03	11.78 ± 0.37	3386.7	46.9	76.51
PKS 1502+036	2.63 ± 0.05	4.53 ± 0.35	434.8	46.1	2.53 ± 0.10	0.06 ± 0.05	4.29 ± 0.39	434.4	46.0	1.90
PKS 2004-447	2.38 ± 0.09	1.42 ± 0.24	106.1	45.2	1.54 ± 0.36	0.42 ± 0.18	0.91 ± 0.23	113.1	45.3	10.10

^a The γ -ray flux values in units of $10^{-8} \text{ ph cm}^{-2} \text{ s}^{-1}$.

^b The PL and LP luminosities at logarithmic scale.

discovery of this source in the γ -ray band, the photon index is found to be 1.93 ± 0.09 , which is typical of high-synchrotron peaked blazars (Ackermann et al. 2011). Similar behavior was reported earlier by D’Ammando et al. (2012). The photon index of PMN J0948+0022 is also found to be harder during the high-activity periods. During its first outburst in 2010 July, a photon index of 2.39 ± 0.12 was obtained, which is harder when compared to the five-year average value of 2.62 ± 0.02 . This result is similar to that first reported by Foschini et al. (2011b). A maximum flux of $(1.21 \pm 0.36) \times 10^{-7} \text{ ph cm}^{-2} \text{ s}^{-1}$ is observed from PKS 1502+036 in the bin centered at MJD 55,477. The corresponding photon index during this period is 2.83 ± 0.28 , which is not significantly different from its five-year average value of 2.63 ± 0.05 . The spectral evolution of PKS 2004-447 could not be ascertained owing to its faintness. Overall, however, there are hints of spectral hardening for three out of the five γ -NLSy1 galaxies during flares, as compared to their five-year average behavior. No strong spectral change is noticed on shorter timescales. These results are in line with the findings of Abdo et al. (2010d) and Foschini et al. (2012).

To study the overall spectral behavior of these sources, in Figure 7 we plot the photon index against the flux, as obtained from the light curve analysis. PKS 1502+036 shows a softer when brighter behavior, whereas no conclusion can be drawn about PKS 2004-447 because of the small number of data points. Similar results have been reported by Paliya et al. (2013b). Moreover, the remaining three sources seem to show a softer when brighter trend, up to a flux level of $\simeq 1.5 \times 10^{-7} \text{ ph cm}^{-2} \text{ s}^{-1}$. Above this flux value, these sources may hint at a harder when brighter trend. To statistically test these behaviors, we perform a Monte Carlo test that takes into account of the dispersion in flux and photon index measurements. For each observed pair of flux and index values, we re-sample by extracting the data from a normal distribution centered on the observed value and standard deviation equal to the 1σ error estimate. We do not perform this test on the data of PKS 1502+036 and PKS 2004-447 due to their small sample size. For lower fluxes (i.e., $F_\gamma < 1.5 \times 10^{-7} \text{ ph cm}^{-2} \text{ s}^{-1}$), the correlation coefficients (ρ) are found to be 0.21, 0.26, and 0.27 with 95% confidence limits of $-0.27 \leq \rho \leq 0.61$, $-0.03 \leq \rho \leq 0.51$, and $-0.05 \leq \rho \leq 0.54$, respectively, for 1H 0323+342, SBS 0846+513, and PMN J0948+0022. On the other hand, for higher fluxes ($F_\gamma > 1.5 \times 10^{-7} \text{ ph cm}^{-2} \text{ s}^{-1}$), the correlation coefficients are -0.32 , -0.09 , and -0.08 , with 95% confidence limits of $-0.67 \leq \rho \leq 0.14$, $-0.48 \leq \rho \leq 0.33$, and $-0.27 \leq \rho \leq 0.12$, respectively, for 1H 0323+342, SBS 0846+513, and PMN J0948+0022. Clearly, based on the Monte Carlo analysis, it is difficult to claim a correlation between fluxes and photon indices.

4.4. Origin of Spectral Curvature/Break

The origin of the γ -ray spectral break detected by *Fermi*-LAT in many FSRQs is still an open question. Many theoretical models are available in the literature to explain the observed spectral break. One among the extrinsic causes could be due to the attenuation of γ -rays by photon-photon pair production on He II Lyman recombination lines within the BLR, as explained by the double-absorber model of Poutanen & Stern (2010). In this model, the γ -ray dissipation region should lie inside the BLR. However, by analyzing a sample of γ -ray bright blazars, Harris et al. (2012) have raised questions about the validity of the double-absorber model. The break energy predicted by this model is found to be inconsistent with observations. Finke & Dermer (2010) proposed a scenario wherein the observed spectral break could be explained as the sum of hybrid scattering of the accretion disk and BLR photons, but this solution requires a wind-like profile for the BLR. Using an equipartition approach, Cerruti et al. (2013) proposed a scenario in which the break in the GeV spectra occurs as a consequence of the Klein-Nishina (KN) effect on the Compton scattering of BLR photons by relativistic electrons having a curved particle distribution in the jet. Alternatively, the γ -ray spectral break can also result from intrinsic effects. In this intrinsic model, the break can happen if there is a cutoff in the energy distribution of particles that produce the γ -ray emission (Abdo et al. 2009b).

Three out of the five γ -NLSy1 galaxies studied here—1H 0323+342, SBS 0846+513 and PMN J0948+0022—show clear deviation from a simple PL model. Instead, the LP model seems to describe the data better. From the SED modeling of 1H 0323+342 and PMN J0948+0022, Abdo et al. (2009d) constrained their γ -ray emission region to be well inside the BLR (see also Foschini et al. 2012; Paliya et al. 2014). In such a scenario, the presence of the curvature in the γ -ray spectrum of these two sources can be explained on the basis of the KN effect. This is because the UV photons produced by the accretion disk and reprocessed by the BLR are blueshifted by a factor $\sim \Gamma$. Assuming a typical value of $\Gamma \simeq 10$, the approximate energy of these photons in the rest frame of the blob is about 10^{16} Hz , and hence the IC scattering with the electrons (having $\gamma \simeq 1000$) occurs under the mild KN regime. This hypothesis can also be tested by determining the energy of the highest energy photons detected by *Fermi*-LAT. The detection of very high energy photons ($>$ few tens of GeV) will clearly rule out the possibility that the emission region is located inside the BLR. We used `gtsrcprob` tool to determine the energy of the highest energy photon. This value is 32.7 GeV (95.76% detection probability) and 4.71 GeV (98.15% detection probability) for 1H 0323+342 and PMN

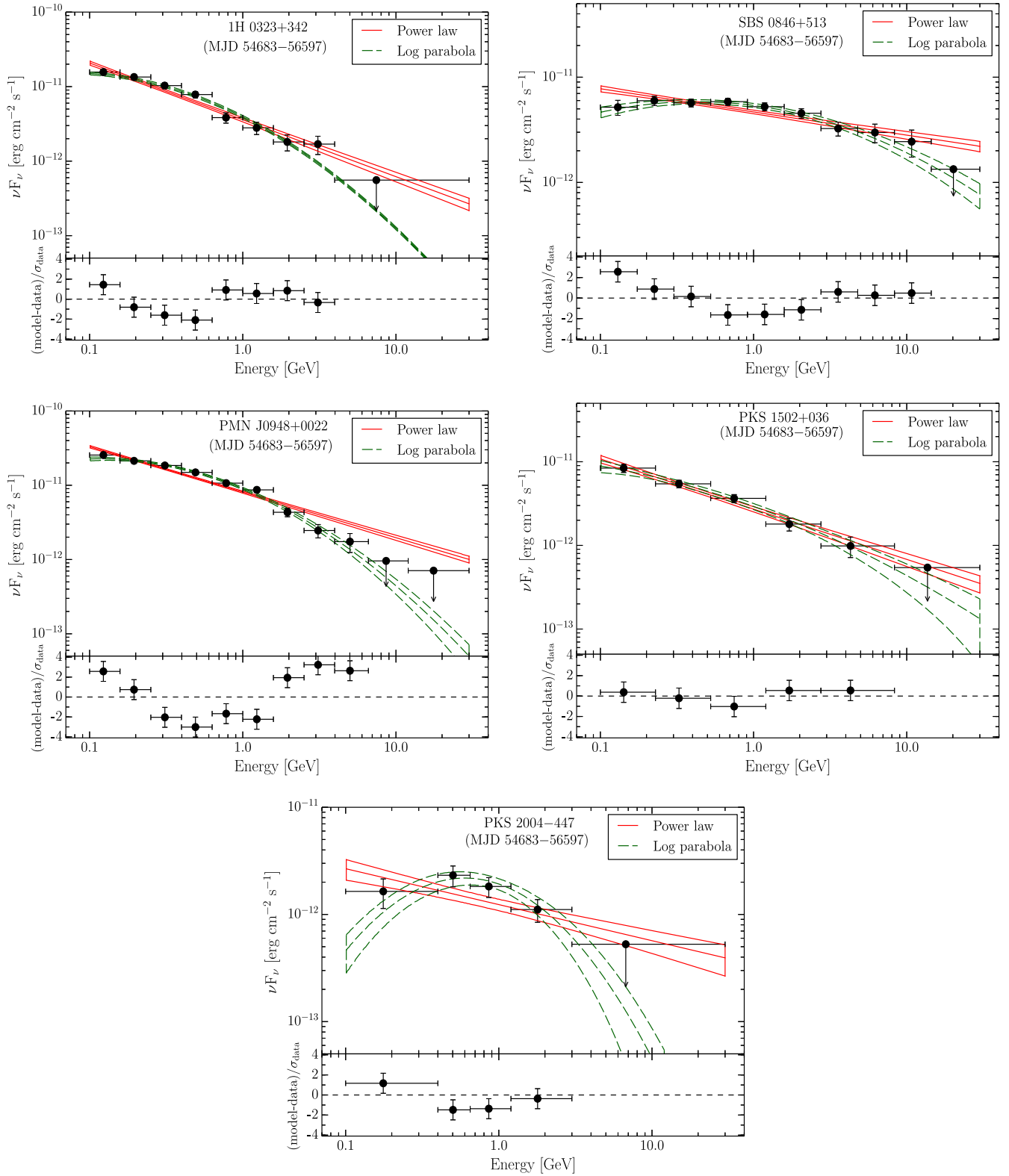


Figure 4. Five-year average *Fermi*-LAT SED of the γ -NLSy1 galaxies. Solid and dashed lines represent PL and LP model fits, respectively, with uncertainties. The residuals in the lower panels refer to the PL model.

J0948+0022, respectively. The highest photon energy for 1H 0323+342 closely satisfies the BLR γ -ray transparency condition (Ghisellini & Tavecchio 2009), and thus the origin of the γ -ray emission could lie inside the BLR. We note here that the non-detection of very high energy γ -ray photons does

not ensure that the emission region is located inside the BLR, but such a detection would definitely rule out this possibility.

The γ -ray emission from SBS 0846+513 is well modeled by IC scattering of dusty torus photons (D’Ammando et al. 2013a) and this sets the location of the γ -ray emission region to be

Table 4
Details of the PL and LP Model Fits to the Various Brightness States of the γ -NLSy1 Galaxies. The Units are Same as in Table 3

Activity State (MJD)	PL				LP					
	Γ_γ	$F_{0.1-300\text{ GeV}}$	TS	Log L _{PL}	α	β	$F_{0.1-300\text{ GeV}}$	TS	Log L _{LP}	TS_{curve}
				1H 0323+342						
H1 (54683–56200)	2.83 ± 0.07	5.44 ± 0.46	291.8	44.3	2.70 ± 0.09	0.34 ± 0.11	4.89 ± 0.43	301.7	44.2	16.13
H2 (56200–56400)	2.67 ± 0.08	12.90 ± 1.23	222.0	44.7	2.49 ± 0.12	0.21 ± 0.09	11.60 ± 1.28	228.0	44.6	7.68
H3 (56400–56550)	2.68 ± 0.07	18.50 ± 1.51	335.2	44.9	2.62 ± 0.09	0.08 ± 0.06	17.80 ± 1.56	335.0	44.7	1.61
				SBS 0846+513						
S1 (55716–55746)	1.99 ± 0.01	21.90 ± 0.52	608.6	47.6	1.21 ± 0.01	0.32 ± 0.01	15.60 ± 0.22	634.8	47.8	29.53
S2 (56018–56170)	2.14 ± 0.05	12.20 ± 0.90	917.0	47.2	1.92 ± 0.09	0.09 ± 0.03	10.80 ± 0.95	919.3	47.2	6.87
S3 (56390–56597)	2.24 ± 0.05	12.20 ± 0.81	983.9	47.1	2.08 ± 0.08	0.07 ± 0.03	11.20 ± 0.87	981.5	47.1	5.20
				PMN J0948+0022						
P1 (54683–55200)	2.67 ± 0.05	11.70 ± 0.63	842.9	46.9	2.40 ± 0.08	0.21 ± 0.05	10.70 ± 0.62	866.0	46.9	21.72
P2 (55300–55450)	2.54 ± 0.06	14.40 ± 1.22	323.2	47.1	2.14 ± 0.17	0.26 ± 0.06	12.20 ± 2.13	331.2	47.0	12.02
P3 (56200–56350)	2.62 ± 0.01	24.00 ± 0.47	756.9	47.3	2.44 ± 0.01	0.14 ± 0.01	22.60 ± 0.19	764.5	47.2	7.65

outside the BLR, where IC scattering takes place under the Thomson regime. Thus the most probable cause of the curvature/break in the γ -ray spectrum would be intrinsic to the emitting particle distribution. In this picture, the curvature must be visible in the γ -ray spectrum of SBS 0846+513 in all brightness states. However, the poor photon statistics hinder us from detecting this curvature. Additionally, if the observed curvature is caused by the curved particle energy distribution, a similar feature should be seen in the optical/UV part of the spectrum, provided that the optical/UV part is dominated by the synchrotron radiation. Hence, a dedicated multi-wavelength study similar to that done for 3C 454.3 (Cerruti et al. 2013), is desired to test these possible scenarios.

4.5. Gamma-ray Loud NLSy1 Galaxies versus Gamma-ray Loud Blazars

The γ -ray spectral curvature observed in some of the γ -NLSy1 galaxies studied here are commonly known in *Fermi*-LAT detected FSRQs (Abdo et al. 2010d). Such breaks are also noticed in the LAT spectra of a few low and intermediate synchrotron peaked BL Lac objects. In the BL Lac objects where a γ -ray spectral break is observed, broad optical emission lines are reported in the quiescent states of few of them. The sources AO 0235+164 (Raïteri et al. 2007) and PKS 0537–441 (Ghisellini et al. 2011) are good examples of this. It is likely that these BL Lac objects could belong to the FSRQ class of AGN as noted by Ghisellini et al. (2011). Moreover, there are observations of curvature in the X-ray spectra of many high-frequency peaked BL Lac objects (Massaro et al. 2011, and references therein), but the presence of curvature in their γ -ray spectra is yet to be verified. Therefore, based on the available observations it is likely that the γ -ray spectral break is a characteristic feature of the FSRQ class of AGN.

All five sources studied here have steep photon indices (Table 3) and the average value is 2.55 ± 0.03 . This is similar to the average photon index for FSRQs (2.42 ± 0.17) in the 2LAC (Ackermann et al. 2011), and is steeper than the value of 2.17 ± 0.12 , 2.13 ± 0.14 , and 1.90 ± 0.17 for the low, intermediate, and high synchrotron peaked BL Lac objects, respectively. Thus, in terms of the average γ -ray photon index, these γ -NLSy1 galaxies are similar to FSRQs. However, the

γ -ray luminosities of these five γ -NLSy1 galaxies are lower when compared to powerful FSRQs, but higher than BL Lac objects (e.g., Figure 6 of Paliya et al. 2013b). As some of the γ -NLSy1 galaxies studied here show evidence of the presence of spectral curvature and high flux variability, we argue based on the γ -ray properties, that these sources show resemblance to FSRQs.

Positioning the FSRQs and BL Lac objects detected during the first three months of the *Fermi* operation (Abdo et al. 2009a) on the γ -ray luminosity (L_γ) versus γ -ray spectral index (α_γ) diagram, Ghisellini et al. (2009) have postulated the existence of low BH mass FSRQs having steep α_γ and low L_γ . In the L_γ v/s α_γ plane, the five γ -NLSy1 galaxies studied here tend to have steep α_γ values. Their L_γ values are intermediate to the FSRQ 3C 454.3 and the BL Lac object Mrk 421 (Paliya et al. 2013b). Further, from the estimates of BH masses available in the literature, it is also found that these γ -NLSy1 galaxies host low mass BHs (Table 1). They appear to be on the higher side of the BH masses known for NLSy1 galaxies in general (Komossa et al. 2006; Yuan et al. 2008), but lower than that known for powerful blazars (Ghisellini et al. 2010). Thus it is likely that these γ -NLSy1 galaxies are the low BH mass FSRQs already predicted by Ghisellini et al. (2009). However, we note that the estimation of the BH mass of NLSy1 galaxies is still a matter of debate. For example, using the virial relationship Yuan et al. (2008) reported the central BH mass of PMN J0948+0022 as $\sim 10^{7.5} M_\odot$, whereas using the SED modeling approach Abdo et al. (2009d) found $\sim 10^{8.2} M_\odot$. Recently Calderone et al. (2013) obtained a BH mass of this source as large as $\sim 10^{9.2} M_\odot$. Further, on examination of the SEDs of the five γ -NLSy1 galaxies—1H 0323+342 (Paliya et al. 2014), SBS 0846+513 (D’Ammando et al. 2012), PMN J0948+0022 (Foschini et al. 2011b), PKS 1502+036, and PKS 2004–447 (Paliya et al. 2013b)—we find that they all have Compton dominance (which is the ratio of inverse Compton to synchrotron peak luminosities in the SED) of the order of ~ 10 similar to that known for powerful FSRQs.

5. CONCLUSIONS

In this paper, we present the detailed analysis of the γ -ray temporal and spectral behavior of the five RL-NLSy1 galaxies

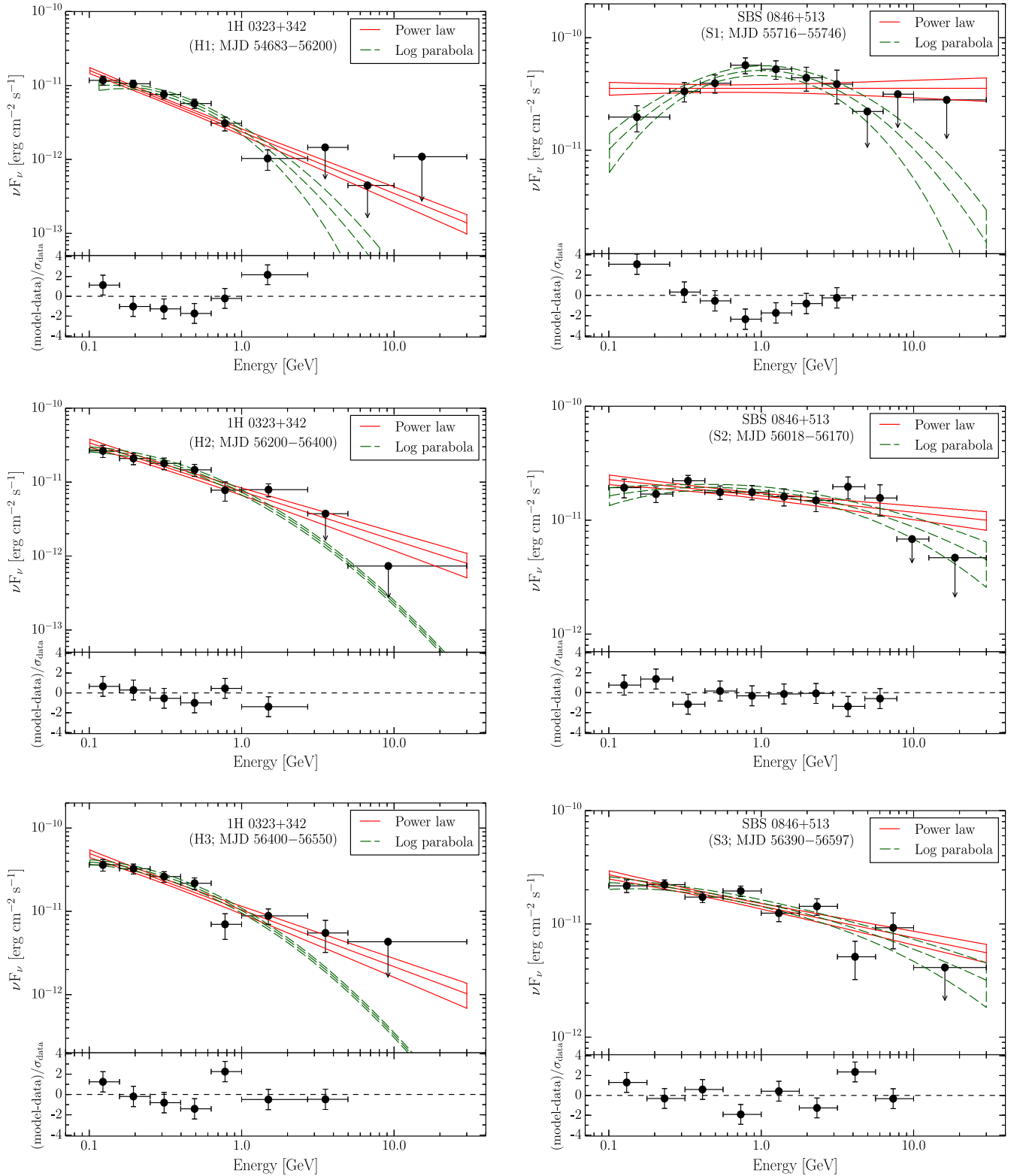


Figure 5. *Fermi*-LAT SED of 1H 0323+342 (left panels) and SBS 0846+513 (right panels) in their different brightness states. Other information is same as in Figure 4.

that are detected by *Fermi*-LAT with high significance. We summarize our main results as follows:

1. During the period 2008 August to 2013 November, three out of five γ -NLSy1 galaxies show significant flux

variations. The same cannot be claimed for the remaining two sources due to their faintness and/or intrinsic low variability nature. The F_{var} values obtained are 0.498 ± 0.046 , 0.467 ± 0.042 , and 0.443 ± 0.029 for 1H 0323 +342, SBS 0846+513, and PMN J0948+0022,

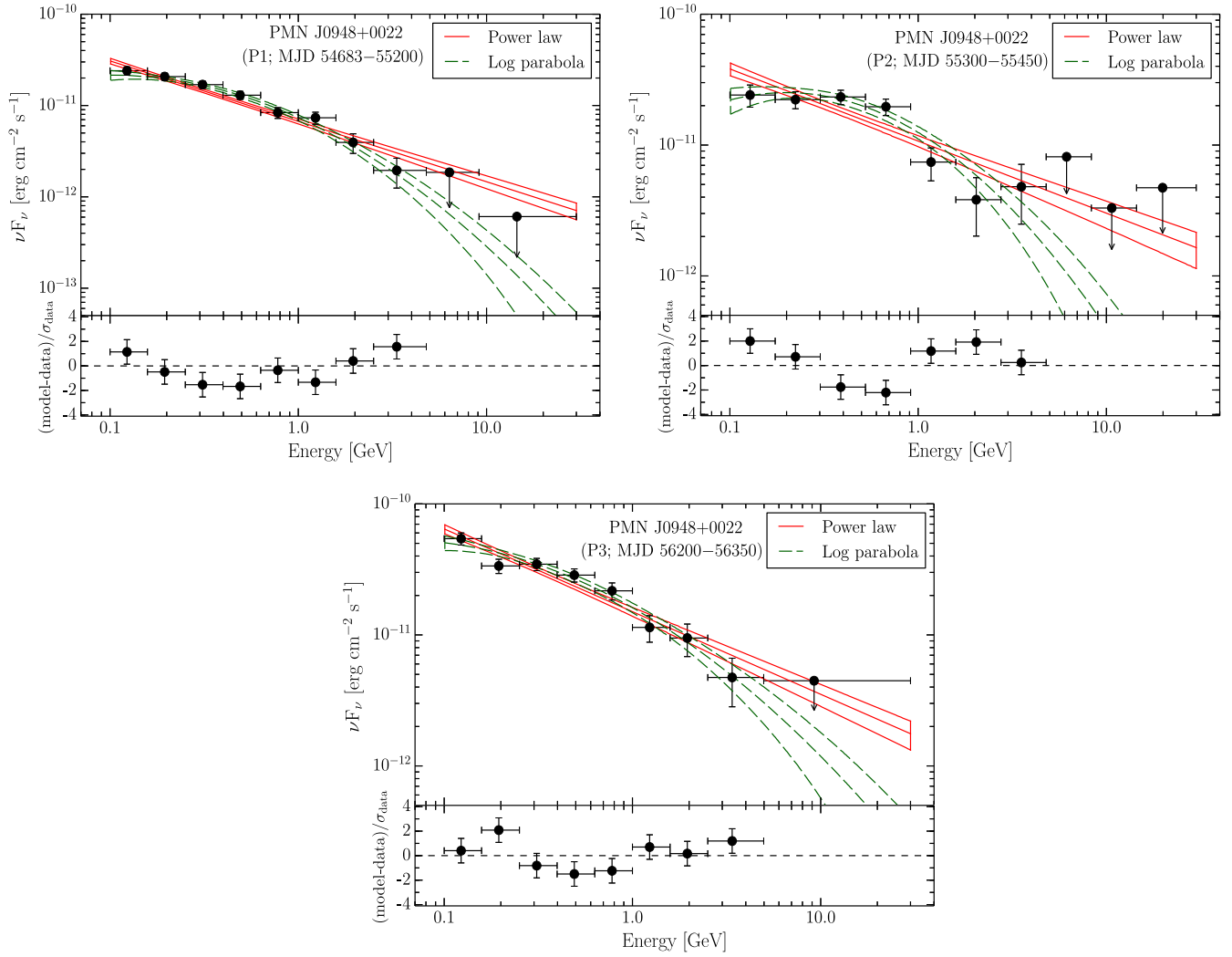


Figure 6. *Fermi*-LAT SED of PMN J0948+0022 during its different activity states. Other information are same as in Figure 4.

- respectively. These are larger than that reported for FSRQs (0.24 ± 0.01) and BL Lac objects (0.12 ± 0.01 , 0.07 ± 0.02 , and 0.07 ± 0.02 for LSP, ISP, and HSP BL Lac objects, respectively) by Abdo et al. (2010c). This supports the idea that in terms of the γ -ray flux variations these sources are similar to the FSRQ class of AGN. More than one episode of flaring activity is seen in 1H 0323+342, SBS 0846+513, and PMN J0948+0022, whereas no such flaring activities are observed in PKS 1502+342 and PKS 2004–447. Results from a Monte Carlo simulation to test for the presence of a possible correlation between the fluxes and photon indices do not support for any correlation at lower or higher flux levels.
2. The observed average MeV–GeV γ -ray energy spectra of 1H 0323+342 and PMN J0948+0022 show significant deviation from a simple PL model. The data are well fit with the LP model. A hint for the presence of a curvature is found for SBS 0846+513. For PKS 1502+036 and PKS 2004–447, the PL model fits the observations very well.
 3. Three sources—1H 0323+342, SBS 0846+513, and PMN J0948+0022—have shown flux variations in their γ -ray emission thereby enabling us to study their spectral behavior in different brightness states. Again, the PL model does not well represent the observed spectra in some of their activity states. A statistically significant

curvature is observed in the low, high, and moderately active state γ -ray spectra of 1H 0323+342, SBS 0846+513, and PMN J0948+0022, respectively.

4. The SED modeling of 1H 0323 + 342 and PMN J0948 + 0022 by Abdo et al. (2009d) leads to the conclusion that the location of γ -ray emission in these sources is inside the BLR (see also, Foschini et al. 2012; Paliya et al. 2014). It is thus likely that the observed γ -ray emission in these sources is due to IC scattering of BLR photons occurring under the KN regime. In such a scenario a prominent curvature in the γ -ray spectra is expected (see Abdo et al. 2010a, for a similar argument). For SBS 0846 +513, the γ -ray emission is well modeled by IC scattering of dusty torus photons (D’Ammando et al. 2013a). Because the production of γ -rays would be in the Thomson regime, the observed curvature could be intrinsic to the source and can be attributed to the break/curvature in the particle energy distribution.
5. The average photon indices of the γ -NLSy1 galaxies obtained from the PL fits have values ranging between 2.2 and 2.8. This matches well with the average photon index (2.42 ± 0.17) found for FSRQs in the 2LAC. However, these values are softer when compared to BL Lac objects (Ackermann et al. 2011).

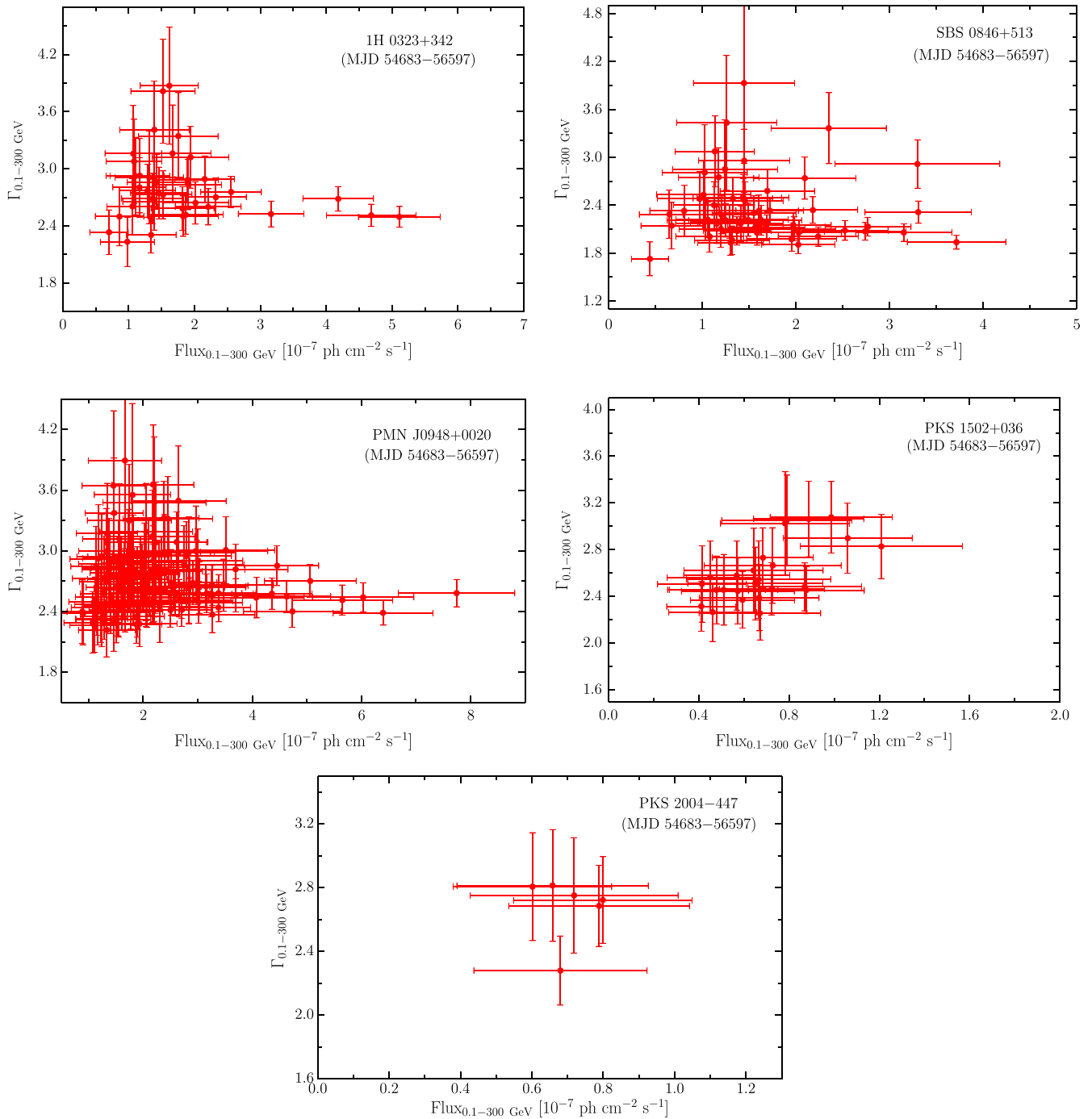


Figure 7. Photon index vs. γ -ray flux plots, obtained from long-term light curve analysis.

With the accumulation of more data by *Fermi* in the future and subsequent generation of high-quality γ -ray spectra, it will be possible to further constrain various models proposed for the origin of the MeV–GeV break and other γ -ray spectral properties of the γ -NLSy1 galaxies. As observed by Abdo et al. (2010d) and Tanaka et al. (2011), a break in the γ -ray spectrum is a characteristic feature of powerful FSRQs, which is also clearly visible in γ -NLSy1 galaxies. The origin of this curvature and break in their spectra could be different physical mechanisms taking place at different regions and at different scales. The overall observed properties of these γ -NLSy1 galaxies indicate that they could be similar to powerful FSRQs, but with low or moderate jet power (see Abdo et al. 2009d;

D’Ammando et al. 2013a; Paliya et al. 2013b for a comparison).

We thank the referee for constructive comments that improved the presentation significantly. Use of *Hydra* cluster at the Indian Institute of Astrophysics is also acknowledged. C. D.R. acknowledges IUCAA for its assistance through the visiting associateship program.

REFERENCES

- Abdo, A. A., Ackermann, M., Ajello, M., et al. 2009a, *ApJ*, 700, 597
 Abdo, A. A., Ackermann, M., Ajello, M., et al. 2009b, *ApJ*, 699, 817

- Abdo, A. A., Ackermann, M., Ajello, M., et al. 2009c, *ApJ*, 699, 976
- Abdo, A. A., Ackermann, M., Ajello, M., et al. 2009d, *ApJL*, 707, L142
- Abdo, A. A., Ackermann, M., Agudo, I., et al. 2010a, *ApJ*, 721, 1425
- Abdo, A. A., Ackermann, M., Ajello, M., et al. 2010b, *ApJS*, 188, 405
- Abdo, A. A., Ackermann, M., Ajello, M., et al. 2010c, *ApJ*, 722, 520
- Abdo, A. A., Ackermann, M., Ajello, M., et al. 2010d, *ApJ*, 710, 1271
- Abdo, A. A., Ackermann, M., Ajello, M., et al. 2011, *ApJL*, 733, L26
- Ackermann, M., Ajello, M., Allafort, A., et al. 2011, *ApJ*, 743, 171
- Antón, S., Browne, I. W. A., & Marchã, M. J. 2008, *A&A*, 490, 583
- Atwood, W. B., Abdo, A. A., Ackermann, M., et al. 2009, *ApJ*, 697, 1071
- Boller, T., Brandt, W. N., & Fink, H. 1996, *A&A*, 305, 53
- Brown, A. M. 2013, *MNRAS*, 431, 824
- Calderone, G., Foschini, L., Ghisellini, G., et al. 2011, *MNRAS*, 413, 2365
- Calderone, G., Ghisellini, G., Colpi, M., & Dotti, M. 2013, *MNRAS*, 431, 210
- Carpenter, B., & Ojha, R. 2013, *ATel*, 5344, 1
- Cerruti, M., Dermer, C. D., Lott, B., Boisson, C., & Zech, A. 2013, *ApJL*, 771, L4
- D'Ammando, F., & Ciprini, S. 2011, *ATel*, 3429, 1
- D'Ammando, F., & Orienti, M. 2013, *ATel*, 4694, 1
- D'Ammando, F., Orienti, M., Finke, J., et al. 2012, *MNRAS*, 426, 317
- D'Ammando, F., Orienti, M., Finke, J., et al. 2013a, *MNRAS*, 436, 191
- D'Ammando, F., Orienti, M., Doi, A., et al. 2013b, *MNRAS*, 433, 952
- Doi, A., Nagai, H., Asada, K., et al. 2006, *PASJ*, 58, 829
- Doi, A., Nagira, H., Kawakatu, N., et al. 2012, *ApJ*, 760, 41
- Donato, D. 2010, *ATel*, 2733, 1
- Donato, D., & Perkins, J. S. 2011, *ATel*, 3452, 1
- Finke, J. D., & Dermer, C. D. 2010, *ApJL*, 714, L303
- Foschini, L. 2011, in Proc. Science 126, Narrow-Line Seyfert 1 Galaxies and their Place in the Universe, ed. L. Foschini, M. Colpi, L. Gallo, et al. (PoS (NLSI)024), http://pos.sissa.it/cai-bin/reader/conf_cai?confid=126
- Foschini, L., Ghisellini, G., et al. Fermi/Lat Collaboration 2010 in ASP Conf. Ser. 427, Accretion and Ejection in AGN: a Global View, ed. L. Maraschi, G. Ghisellini, R. della Ceca, & F. Tavecchio (San Francisco, CA: ASP), 243
- Foschini, L., Ghisellini, G., Tavecchio, F., Bonnoli, G., & Stamerra, A. 2011a, *A&A*, 530, A77
- Foschini, L., Ghisellini, G., Kovalev, Y. Y., et al. 2011b, *MNRAS*, 413, 1671
- Foschini, L., Angelakis, E., Fuhrmann, L., et al. 2012, *A&A*, 548, A106
- Fossati, G., Maraschi, L., Celotti, A., Comastri, A., & Ghisellini, G. 1998, *MNRAS*, 299, 433
- Gasparrini, D., & Cutini, S. 2011, *ATel*, 3579, 1
- Ghisellini, G., Maraschi, L., & Tavecchio, F. 2009, *MNRAS*, 396, L105
- Ghisellini, G., & Tavecchio, F. 2009, *MNRAS*, 397, 985
- Ghisellini, G., Tavecchio, F., Foschini, L., & Ghirlanda, G. 2011, *MNRAS*, 414, 2674
- Ghisellini, G., Tavecchio, F., Foschini, L., et al. 2010, *MNRAS*, 402, 497
- Goodrich, R. W. 1989, *ApJ*, 342, 224
- Grupe, D., & Mathur, S. 2004, *ApJL*, 606, L41
- Harris, J., Daniel, M. K., & Chadwick, P. M. 2012, *ApJ*, 761, 2
- Hayashida, K. 2000, *NewAR*, 44, 419
- Ikejiri, Y., Uemura, M., Sasada, M., et al. 2011, *PASJ*, 63, 639
- Itoh, R., Tanaka, Y. T., Fukazawa, Y., et al. 2013, *ApJL*, 775, L26
- Jiang, N., Zhou, H.-Y., Ho, L. C., et al. 2012, *ApJL*, 759, L31
- Komossa, S., Voges, W., Xu, D., et al. 2006, *AJ*, 132, 531
- Kraft, R. P., Burrows, D. N., & Nousek, J. A. 1991, *ApJ*, 374, 344
- Laor, A. 2000, *ApJL*, 543, L111
- Leighly, K. M. 1999a, *ApJS*, 125, 297
- Leighly, K. M. 1999b, *ApJS*, 125, 317
- León Tavares, J., Kotilainen, J., Chavushyan, V., et al. 2014, *ApJ*, 795, 58
- Liu, H., Wang, J., Mao, Y., & Wei, J. 2010, *ApJL*, 715, L113
- Marscher, A. P. 2009, arXiv:0909.2576
- Massaro, F., Paggi, A., Elvis, M., & Cavaliere, A. 2011, *ApJ*, 739, 73
- Mattox, J. R., Bertsch, D. L., Chiang, J., et al. 1996, *ApJ*, 461, 396
- Nemmen, R. S., Georganopoulos, M., Guiriec, S., et al. 2012, *Sci*, 338, 1445
- Nolan, P. L., Abdo, A. A., Ackermann, M., et al. 2012, *ApJS*, 199, 31
- Oshlack, A. Y. K. N., Webster, R. L., & Whiting, M. T. 2001, *ApJ*, 558, 578
- Osterbrock, D. E., & Pogge, R. W. 1985, *ApJ*, 297, 166
- Paliya, V. S., Sahayanathan, S., Parker, M. L., et al. 2014, *ApJ*, 789, 143
- Paliya, V. S., Stalin, C. S., Kumar, B., et al. 2013, *MNRAS*, 428, 2450
- Paliya, V. S., Stalin, C. S., Shukla, A., & Sahayanathan, S. 2013, *ApJ*, 768, 52
- Peterson, B. M., McHardy, I. M., Wilkes, B. J., et al. 2000, *ApJ*, 542, 161
- Pounds, K. A., Done, C., & Osborne, J. P. 1995, *MNRAS*, 277, L5
- Poutanen, J., & Stern, B. 2010, *ApJL*, 717, L118
- Raiteri, C. M., Villata, M., Capetti, A., et al. 2007, *A&A*, 464, 871
- Saito, S., Stawarz, Ł., Tanaka, Y. T., et al. 2013, *ApJL*, 766, L11
- Sikora, M., Madejski, G., Moderski, R., & Poutanen, J. 1997, *ApJ*, 484, 108
- Tanaka, Y. T., Stawarz, Ł., Thompson, D. J., et al. 2011, *ApJ*, 733, 19
- Tavecchio, F., Ghisellini, G., Bonnoli, G., & Ghirlanda, G. 2010, *MNRAS*, 405, L94
- Thompson, D. J., Bertsch, D. L., Fichtel, C. E., et al. 1993, *ApJS*, 86, 629
- Urry, C. M., & Padovani, P. 1995, *PASP*, 107, 803
- Vaughan, S., Edelson, R., Warwick, R. S., & Uttley, P. 2003, *MNRAS*, 345, 1271
- Véron-Cetty, M.-P., & Véron, P. 2010, *A&A*, 518, A10
- Wang, T., Brinkmann, W., & Bergeron, J. 1996, *A&A*, 309, 81
- Xu, D., Komossa, S., Zhou, H., et al. 2012, *AJ*, 143, 83
- Yuan, W., Zhou, H. Y., Komossa, S., et al. 2008, *ApJ*, 685, 801
- Zhou, H., Wang, T., Yuan, W., et al. 2006, *ApJS*, 166, 128